Self-energy of the $n=2$ states in a strong Coulomb field

Peter J. Mohr
Gibbs Laboratory, Physics Department, Yale University, New Haven, Connecticut 06520
(Received 16 June 1982)

A calculation of the self-energy radiative correction to the energy level of an electron in the $2S_{1/2}$, $2P_{1/2}$, or $2P_{3/2}$ state in a Coulomb field, with nuclear charge Z in the range 10—110, is described.

I. INTRODUCTION

This paper describes a calculation of the self-energy radiative correction of order α to the energy levels of the $2S_{1/2}$, $2P_{1/2}$, and $2P_{3/2}$ states for an electron in a strong Coulomb field. The self-energy correction is the real part of the energy-level shift corresponding to the Feynman diagram in Fig. 1(a). The method of calculation is similar to a method previously employed to evaluate the $1S_{1/2}$-state level shift.[1,2] Results of the calculation for the $2S_{1/2}$ and $2P_{1/2}$ states have been reported previously.[3] In this paper, results for the $2P_{3/2}$-state level shift are reported, and details of the calculation for all $n=2$ states are given. To order α, there is also a vacuum-polarization level shift corresponding to the Feynman diagram in Fig. 1(b).[4] To aid in applications, a tabulation of the Coulomb expectation values of the Uehling potential,[5,6] which gives the dominant vacuum-polarization correction,[4] is included here.

Radiative corrections for $n=2$ states have been calculated to the lowest few orders in $Z\alpha$ (see references in Ref. 1), but to achieve good accuracy at high Z, a calculation that includes all orders in $Z\alpha$ is needed. Evaluation of the radiative corrections is necessary for an accurate theoretical prediction of the energy levels in high-Z hydrogenlike atoms.[7–9] Recent experiments have extended the range of measurements to $Z=17$ and 18.[10,11] The Coulomb-field values also provide a first approximation to both the radiative level shifts in high-Z few-electron atoms[12,13] and the radiative shifts of inner levels of heavy neutral atoms.[14–18] Comparison of theory and experiment in these systems provides an important test of strong-field quantum electrodynamics. These applications and related theoretical work have been reviewed by Brodsky and Mohr.[19]

The self-energy radiative level shift ΔE_n of order α, to all orders in $Z\alpha$, for level n is given by the limit as the regulator parameter $\Lambda\rightarrow\infty$ of

$$\Delta E_n(\Lambda)=\mathrm{Re}(\Delta E_L)+\Delta E_{HA}(\Lambda)+\Delta E_{HB}+\Delta E_M(\Lambda)\ . \tag{1.1}$$

In (1.1), the level shift is written in terms of a low-energy part ΔE_L, a high-energy part $\Delta E_H(\Lambda)$, and the mass renormalization counter term $\Delta E_M(\Lambda)$, as described in Ref. 1. Evaluation of ΔE_L is described in Sec. II. The high-energy part is further divided into two parts $\Delta E_H(\Lambda)=\Delta E_{HA}(\Lambda)+\Delta E_{HB}$ where $\Delta E_{HA}(\Lambda)$ contains both the mass renormalization divergence and the parts of $\Delta E_H(\Lambda)$ that are of order lower than $(Z\alpha)^4$. Evaluation of $\Delta E_{HA}(\Lambda)$ and ΔE_{HB} is discussed in Sec. III and Sec. IV, respectively. The results of the self-energy calculation are summarized in Sec. V. Coulomb expectation values of the Uehling potential and consistency checks are given in appendices.

II. THE LOW-ENERGY PART ΔE_L

The real part of ΔE_L is given by the principal value integral[1]

$$\mathrm{Re}(\Delta E_L)=\frac{\alpha}{\pi}E_n-\frac{\alpha}{\pi}P\int_0^{E_n}dz\int_0^{\infty}dx_2x_2^2\int_0^{\infty}dx_1x_1^2\sum_{\kappa}\sum_{i,j=1}^{2}f_{\hat{i}}(x_2)G_{\kappa}^{ij}(x_2,x_1,z)f_{\hat{j}}(x_1)A_{\kappa}^{ij}(x_2,x_1)\ , \tag{2.1}$$

where $\hat{i}=3-i$ and $\hat{j}=3-j$, and E_n is the Dirac bound-state energy level. Units in which $\hbar$, c, and m_e have unit magnitude are employed. In (2.1), f_i and G_{κ}^{ij} are the components of the Dirac Coulomb radial wave functions and Green's functions, respectively, as defined in Ref. 1 (see also Appendix A). The functions A_{κ}^{ij}, which depend on the bound-state angular-momentum-parity quantum number κ_n as well as the displayed variables,

are given for arbitrary κ_n by Eq. (I3.15) (equation numbers with a prefix I or II refer to equations in Ref. 1 and Ref. 2, respectively.) The special cases of interest here are $S_{1/2}$ states ($\kappa_n=-1$):

$$\begin{aligned}
A_\kappa^{11}(x_2,x_1)&=2(E_n-z)\,|\,\kappa\,|\left[\frac{d}{dy_2}\frac{d}{dy_1}+\frac{\kappa^2-1}{y_2y_1}\right]j_{l(\kappa)}(y_2)j_{l(\kappa)}(y_1)\,,\\
A_\kappa^{12}(x_2,x_1)&=2(E_n-z)\kappa\frac{d}{dy_2}j_{l(\kappa)}(y_2)j_{l(-\kappa)}(y_1)\,,\\
A_\kappa^{21}(x_2,x_1)&=2(E_n-z)\kappa\frac{d}{dy_1}j_{l(-\kappa)}(y_2)j_{l(\kappa)}(y_1)\,,\\
A_\kappa^{22}(x_2,x_1)&=2(E_n-z)\,|\,\kappa\,|\,j_{l(-\kappa)}(y_2)j_{l(-\kappa)}(y_1)\,;
\end{aligned}\tag{2.2}$$

$P_{1/2}$ states ($\kappa_n=1$):

$$\begin{aligned}
A_\kappa^{11}(x_2,x_1)&=2(E_n-z)\,|\,\kappa\,|\,j_{l(\kappa)}(y_2)j_{l(\kappa)}(y_1)\,,\\
A_\kappa^{12}(x_2,x_1)&=-2(E_n-z)\kappa\frac{d}{dy_1}j_{l(\kappa)}(y_2)j_{l(-\kappa)}(y_1)\,,\\
A_\kappa^{21}(x_2,x_1)&=-2(E_n-z)\kappa\frac{d}{dy_2}j_{l(-\kappa)}(y_2)j_{l(\kappa)}(y_1)\,,\\
A_\kappa^{22}(x_2,x_1)&=2(E_n-z)\,|\,\kappa\,|\left[\frac{d}{dy_2}\frac{d}{dy_1}+\frac{\kappa^2-1}{y_2y_1}\right]j_{l(-\kappa)}(y_2)j_{l(-\kappa)}(y_1)\,;
\end{aligned}\tag{2.3}$$

and $P_{3/2}$ states ($\kappa_n=-2$):

$$\begin{aligned}
A_\kappa^{11}(x_2,x_1)=3(E_n-z)\,|\,\kappa\,|\,\Bigg\{&\left[\frac{(\kappa+1)^2(2\kappa^2-\kappa+1)}{y_2^2y_1^2}-\kappa(\kappa+1)\left[\frac{1}{y_2^2}+\frac{1}{y_1^2}\right]+\frac{2}{3}\right]\\
&-\left[\frac{(5\kappa-1)(\kappa+1)}{y_2^2}-2\right]\frac{1}{y_1}\frac{d}{dy_1}-\left[\frac{(5\kappa-1)(\kappa+1)}{y_1^2}-2\right]\frac{1}{y_2}\frac{d}{dy_2}\\
&+[(2\kappa-1)(\kappa+1)+6]\frac{1}{y_2y_1}\frac{d}{dy_2}\frac{d}{dy_1}\Bigg\}j_{l(\kappa)}(y_2)j_{l(\kappa)}(y_1)\,,\\
A_\kappa^{12}(x_2,x_1)=(E_n-z)\,|\,\kappa\,|\,\Bigg[&\left[\left[2\frac{d}{dy_2}+\frac{\kappa-1}{y_2}\right]\frac{\kappa-1}{y_1}j_{l(-\kappa)}(y_2)j_{l(-\kappa)}(y_1)\right.\\
&\left.+\left[2+\frac{6}{y_2}\frac{d}{dy_2}-3\frac{\kappa(\kappa+1)}{y_2^2}\right]j_{l(\kappa)}(y_2)j_{l(\kappa)}(y_1)\right]\,,\\
A_\kappa^{21}(x_2,x_1)=(E_n-z)\,|\,\kappa\,|\,\Bigg[&\left[\frac{\kappa-1}{y_2}\left[2\frac{d}{dy_1}+\frac{\kappa-1}{y_1}\right]j_{l(-\kappa)}(y_2)j_{l(-\kappa)}(y_1)\right.\\
&\left.+\left[2+\frac{6}{y_1}\frac{d}{dy_1}-3\frac{\kappa(\kappa+1)}{y_1^2}\right]j_{l(\kappa)}(y_2)j_{l(\kappa)}(y_1)\right]\,,\\
A_\kappa^{22}(x_2,x_1)=(E_n-z)\,|\,\kappa\,|\left[2\frac{d}{dy_2}\frac{d}{dy_1}+\frac{(2\kappa-1)(\kappa-1)}{y_2y_1}\right]&j_{l(-\kappa)}(y_2)j_{l(-\kappa)}(y_1)\,,
\end{aligned}\tag{2.4}$$

where j_l is the spherical Bessel function with subscript $l(\kappa)=|\,\kappa+\frac{1}{2}\,|-\frac{1}{2}$, and $y_i=(E_n-z)x_i$, $i=1,2$.

The variables of integration in Eq. (2.1) are transformed according to

$$t=1-z/E_n\begin{cases}y=ax_2, & r=x_1/x_2 \quad \text{for } x_2>x_1\\ y=ax_1, & r=x_2/x_1 \quad \text{for } x_2<x_1\end{cases}\tag{2.5}$$

where $a=2(1-E_n^2)^{1/2}$. The low-energy part is then given by

$$\mathrm{Re}(\Delta E_L)=\frac{\alpha}{\pi}[E_n+S_3(\gamma)]\ , \tag{2.6}$$

where

$$S_3(\gamma)=P\int_0^1 dt\int_0^\infty dy\int_0^1 dr\,S(r,y,t,\gamma) \tag{2.7}$$

and

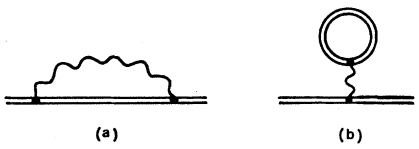

FIG. 1. Feynman diagrams for the lowest-order self-energy (a) and vacuum polarization (b).

$$S(r,y,t,\gamma)=-2E_n a^{-6}r^2y^5\sum_\kappa\sum_{i,j=1}^{2} f_{\hat{i}}(ry/a)G_\kappa^{ij}(ry/a,y/a,E_n(1-t))f_{\hat{j}}(y/a)A_\kappa^{ij}(ry/a,y/a)\ . \tag{2.8}$$

In (2.6) and (2.7) $\gamma=Z\alpha$. This result takes into account the fact that the integrand in (2.1) is systematic under interchange of x_1 and x_2.

The sum over κ in (2.8) is evaluated essentially as described in Ref. 2. In the present case, the method of numerical evaluation of the radial Green's functions $G_\kappa^{ij}(x_2,x_1,z)$ is extended as described in Appendix B to include the region $E(1S_{1/2})<z<E(2P_{3/2})$.

The coordinate integration

$$S_2(t,\gamma)=\int_0^\infty dy\int_0^1 dr\,S(r,y,t,\gamma) \tag{2.9}$$

is evaluated as described in (II 2.16)–(II 2.20) with the general state-dependent definition of q given by

$$q=\frac{1}{2}\left[\frac{2c}{a}-1\right]y\ ,\qquad c=[1-E_n^2(1-t)^2]^{1/2}\ ,\ \mathrm{Re}(c)>0\ . \tag{2.10}$$

In the remaining principal value integration over t,

$$S_3(\gamma)=P\int_0^1 dt\,S_2(t,\gamma)\ , \tag{2.11}$$

it is necessary to deal with the poles of the radial Green's function located at points where $z=E_n(1-t)$ is a bound-state eigenvalue. For the $2S_{1/2}$- and $2P_{1/2}$-state evaluations there is one pole in the integration range located at the $1S_{1/2}$-state eigenvalue $z=E(1S_{1/2})$. For the $2P_{3/2}$-state evaluation, there are poles at both the $1S_{1/2}$-state and $2S_{1/2}$-$2P_{1/2}$-state eigenvalues in the integration range. In all cases, the pole of the Green's function at the upper end point of the range is dominated by a third-order zero in the other factors. To evaluate the principal value integrals, the integration interval is divided into subintervals in such a way that each pole of the integrand is located at the midpoint of a subinterval. The integral over each subinterval containing a pole is evaluated by applying an ordinary Gauss-Legendre formula with an even number of integration points. The fact that this procedure gives the correct principal value integral is demonstrated in Appendix C. In the $2S_{1/2}$- and $2P_{1/2}$-state integrations, the pole is located at $t_1=1-E(1S_{1/2})/E(2S_{1/2})$, and the integration interval is divided into the subintervals $(0,2t_1)$ and $(2t_1,1)$. The integration over t is carried out according to the following prescription:

$$\begin{aligned}
&S_3(\gamma)=S_{31}(\gamma)+S_{32}(\gamma)\ ,\\
&S_{31}(\gamma)=P\int_0^1 dx\,2t_1S_2(2t_1x,\gamma),\quad N=16\\
&S_{32}(\gamma)=\int_0^1 dx\,3x^2(1-2t_1)S_2(2t_1+(1-2t_1)x^3,\gamma),\quad N=13
\end{aligned} \tag{2.12}$$

where N is the number of integration points in the Gauss-Legendre quadrature formula. [The integrals are mapped onto the interval $(-1,1)$ by the appropriate linear variable change.] For the $2P_{3/2}$-state integration, the poles of $S_2(t,\gamma)$ are located at $t_2=1-E(2S_{1/2})/E(2P_{3/2})$ and $t_3=1-E(1S_{1/2})/E(2P_{3/2})$, and the integration subintervals are $(0,2t_2)$, $(2t_2,2t_3-2t_2)$, and $(2t_3-2t_2,1)$. The prescription employed to evaluate the integrals is given by

$$\begin{aligned}
&S_3(\gamma)=S_{31}(\gamma)+S_{32}(\gamma)+S_{33}(\gamma)\ ,\\
&S_{31}(\gamma)=P\int_0^1 dx\,2t_2S_2(2t_2x,\gamma),\quad N=4\\
&S_{32}(\gamma)=P\int_0^1 dx(2t_3-4t_2)S_2(2t_2+(2t_3-4t_2)x,\gamma),\quad N=8\\
&S_{33}(\gamma)=\int_0^1 dx\,3x^2(1-2t_3+2t_2)S_2(2t_3-2t_2+(1-2t_3+2t_2)x^3,\gamma),\quad N=13\ .
\end{aligned} \tag{2.13}$$

The results of the numerical evaluation of $S_3(\gamma)$ appear in Table I. Also listed, in Table II, are values for the function $f_L(\gamma)$ defined by

$$\mathrm{Re}(\Delta E_L)=\frac{\alpha}{\pi}\left[\tfrac{3}{2}\langle\beta\rangle+\tfrac{7}{6}\langle V\rangle+\frac{\gamma^4}{n^3}f_L(\gamma)\right] \tag{2.14}$$

as derived from the corresponding values for $S_3(\gamma)$. (The functions f_L, f_{HA}, f^1_{HA}, h_1, h_2, h_3, h_4, f_{HB}, and F employed in this paper differ by a factor n^{-3}, where n is the principal quantum number of the bound state, from the original functions defined in Ref. 1.) The values for $S_3(\gamma)$ are obtained with the integration prescriptions in (II 2.16), (II 2.20), (2.12), and (2.13) with the number of integration points N listed with each integral replaced by $N+I$, where I is displayed along with the corresponding result in Tables I and II.

A check on the results for $f_L(\gamma)$ is made by comparing the calculated values at the points $Z=10-50$ to the known values at $Z=0$. The small-γ limit is

$$\lim_{\gamma\to 0}[f_L(\gamma)-\tfrac{4}{3}\delta_{l0}\ln(\gamma^{-2})]=C\ , \tag{2.15}$$

where l is the orbital-angular-momentum quantum number for the state, and the values for C, which are deduced independently from the lowest-order (in $Z\alpha$) self-energy calculations as described in Ref. 2, are listed in Table III. The function $\Delta f_L(\gamma)$, defined by

TABLE I. Calculated values for the function S_3.

		$S_3(Z\alpha)$		
Z	I	$2S_{1/2}$	$2P_{1/2}$	$2P_{3/2}$
10	−2	0.498 129 806 190	0.498 111 311 133	0.498 114 990 291
	0	0.498 130 481 221	0.498 111 669 323	0.498 115 349 590
	2	0.498 130 465 672	0.498 111 661 382	0.498 115 341 619
	4	0.498 130 465 255	0.498 111 661 065	0.498 115 341 305
20	0	0.492 635 523 496	0.492 419 419 529	
	2	0.492 635 523 517	0.492 419 419 670	0.492 478 048 953
30	−2	0.483 716 911 856	0.482 846 496 567	0.483 142 268 042
	0	0.483 716 918 695	0.482 846 496 140	0.483 142 285 880
	2	0.483 716 918 740	0.482 846 496 064	0.483 142 287 238
40	2	0.471 572 459 393	0.469 275 647 816	0.470 208 509 625
50	−2	0.456 376 188 639	0.451 558 017 369	0.453 833 654 276
	0	0.456 376 185 971	0.451 558 000 364	0.453 833 751 581
	2	0.456 376 186 507	0.451 558 000 371	0.453 833 757 899
60	2	0.438 268 910 487	0.429 521 518 829	0.434 242 877 428
70	−2	0.417 345 317 668	0.402 980 135 273	0.411 740 644 206
	0	0.417 345 276 748	0.402 980 080 547	0.411 740 829 189
	2	0.417 345 279 154	0.402 980 080 672	0.411 740 822 445
80	2	0.393 627 172 834	0.371 744 692 379	0.386 726 533 714
90	−2	0.367 006 960 282	0.335 639 229 855	0.359 709 129 629
	0	0.367 006 815 022	0.335 639 106 511	0.359 709 128 470
	2	0.367 006 819 538	0.335 639 107 008	0.359 709 013 409
	4			0.359 708 972 648
100	0			0.331 326 331 037
	2	0.337 122 548 595	0.294 522 751 917	0.331 326 104 143
110	−2	0.303 067 361 184	0.248 321 955 071	0.302 366 391 453
	0	0.303 067 135 576	0.248 321 855 802	0.302 366 307 973
	2	0.303 067 135 200	0.248 321 857 042	0.302 365 952 329

TABLE II. Calculated values for f_L.

Z	I	$f_L(Z\alpha)$ $2S_{1/2}$	$2P_{1/2}$	$2P_{3/2}$
10	−2	6.076 095 88	0.858 329 67	0.598 346 01
	0	6.266 533 43	0.959 381 08	0.699 710 20
	2	6.262 146 63	0.957 140 85	0.697 461 48
	4	6.262 029 11	0.957 051 28	0.697 372 91
20	0	4.805 615 97	0.995 206 13	
	2	4.805 616 34	0.995 208 61	0.711 878 75
30	−2	4.081 944 09	1.050 354 37	0.730 231 95
	0	4.081 967 91	1.050 352 88	0.730 294 08
	2	4.081 968 07	1.050 352 62	0.730 298 81
40	2	3.654 071 85	1.122 942 51	0.751 468 26
50	−2	3.390 572 22	1.215 713 00	0.774 774 40
	0	3.390 571 02	1.215 705 33	0.774 818 33
	2	3.390 571 26	1.215 705 33	0.774 821 18
60	2	3.237 888 10	1.333 732 19	0.800 087 92
70	−2	3.173 397 98	1.485 493 30	0.827 154 44
	0	3.173 393 17	1.485 486 87	0.827 176 17
	2	3.173 393 46	1.485 486 88	0.827 175 38
80	2	3.192 292 44	1.685 111 01	0.856 111 65
90	−2	3.306 320 63	1.957 537 91	0.887 020 57
	0	3.306 314 38	1.957 532 60	0.887 020 52
	2	3.306 314 57	1.957 532 62	0.887 015 57
	4			0.887 013 82
100	0			0.920 080 78
	2	3.552 816 50	2.351 004 71	0.920 074 38
110	−2	4.028 836 34	2.973 949 50	0.955 530 18
	0	4.028 831 99	2.973 947 58	0.955 528 58
	2	4.028 831 98	2.973 947 61	0.955 521 72

$$\Delta f_L(\gamma)=f_L(\gamma)-\tfrac{4}{3}\delta_{l0}\ln(\gamma^{-2})-C \qquad (2.16)$$

is plotted in Fig. 2. The calculated values are consistent with the limit $\Delta f_L(0)=0$.

Another check on the calculation of the low-energy part, valid for any Z, is made by examining the imaginary part of the low-energy part $\mathrm{Im}(\Delta E_L)$, which is simply related to the one-photon radiative decay rate of the bound state. This test, described in detail in Appendix D, yields satisfactory results.

TABLE III. Values for the constant C.

State	C
$2S_{1/2}$	−1.1915
$2P_{1/2}$	0.9400
$2P_{3/2}$	0.6900

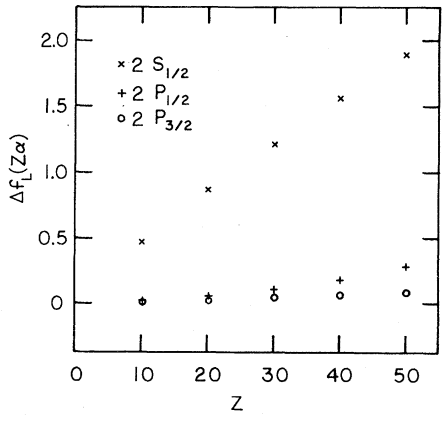

FIG. 2. Calculated values for the function Δf_L.

III. THE HIGH-ENERGY PART $\Delta E_{HA}(\Lambda)$

The high-energy part $\Delta E_{HA}(\Lambda)$ is given by

$$\Delta E_{HA}(\Lambda)=\frac{\alpha}{\pi}\left[\left(\tfrac{3}{4}\ln\Lambda^2-\tfrac{9}{8}\right)\langle\beta\rangle-\tfrac{7}{6}\langle V\rangle+\frac{\gamma^4}{n^3}f_{HA}(\gamma)\right] \tag{3.1}$$

as derived in Ref. 1. The function f_{HA} is the sum

$$f_{HA}(\gamma)=f^1_{HA}(\gamma)+\sum_{i=1}^{4}h_i(\gamma)\ . \tag{3.2}$$

The function f^1_{HA} is

$$\frac{\gamma^4}{n^3}f^1_{HA}(\gamma)=\left[\frac{(1-E_n^2)(3+2E_n^2)}{3E_n^2(1+E_n^2)}-\tfrac{1}{2}\ln 2-\frac{4-9E_n^2+3E_n^4}{4E_n^4}\ln(1+E_n^2)\right]\langle V\rangle$$
$$+\left[\tfrac{9}{4}-\frac{9-3E_n^2}{4E_n^2}\ln(1+E_n^2)\right]\langle(1-\beta/E_n)V\rangle\ . \tag{3.3}$$

The energy and expectation values in (3.3) are explicitly

$$E_n=\left[1+\frac{\gamma^2}{[n-|\kappa|+(\kappa^2-\gamma^2)^{1/2}]^2}\right]^{-1/2}, \tag{3.4a}$$

$$\langle V\rangle=-\frac{\gamma^2}{(\kappa^2-\gamma^2)^{1/2}}\frac{(n-|\kappa|)(\kappa^2-\gamma^2)^{1/2}+\kappa^2}{\{[n-|\kappa|+(\kappa^2-\gamma^2)^{1/2}]^2+\gamma^2\}^{3/2}}\ , \tag{3.4b}$$

$$\langle(1-\beta/E_n)V\rangle=-\frac{\gamma^4}{(\kappa^2-\gamma^2)^{1/2}}\frac{n-|\kappa|}{[n-|\kappa|+(\kappa^2-\gamma^2)^{1/2}]\{[n-|\kappa|+(\kappa^2-\gamma^2)^{1/2}]^2+\gamma^2\}^{3/2}}\ . \tag{3.4c}$$

Here, κ is the angular-momentum-parity quantum number of the bound state. Numerical values for $f^1_{HA}(\gamma)$ are listed in Tables IV–VI. The small-γ limit of $f^1_{HA}(\gamma)$ is

$$f^1_{HA}(0)=\left(\tfrac{5}{3}-\tfrac{7}{4}\ln 2\right)\frac{1}{n}-\left(\tfrac{9}{4}-\tfrac{3}{2}\ln 2\right)\frac{1}{|\kappa|}\ . \tag{3.5}$$

The four functions h_i, $i=1,2,3,4$, are

TABLE IV. Calculated values for f^1_{HA}, h_1, h_2, h_3, h_4, and f_{HA} for the $2S_{1/2}$ state.

Z	$f^1_{HA}(Z\alpha)$	$h_1(Z\alpha)$	$h_2(Z\alpha)$	$h_3(Z\alpha)$	$h_4(Z\alpha)$	$f_{HA}(Z\alpha)$
10	−0.988 462	0.127 250	−0.231 184	0.047 569	−0.362 001	−1.406 829
20	−1.003 798	0.115 839	−0.216 887	0.052 313	−0.358 937	−1.411 471
30	−1.030 396	0.104 631	−0.207 015	0.058 827	−0.360 575	−1.434 529
40	−1.069 984	0.093 039	−0.200 039	0.067 280	−0.366 373	−1.476 077
50	−1.125 389	0.080 399	−0.194 906	0.078 032	−0.376 044	−1.537 909
60	−1.201 096	0.065 905	−0.190 717	0.091 649	−0.389 491	−1.623 751
70	−1.304 319	0.048 495	−0.186 520	0.109 003	−0.406 779	−1.740 121
80	−1.447 140	0.026 636	−0.181 089	0.131 469	−0.428 142	−1.898 267
90	−1.651 160	−0.002 132	−0.172 575	0.161 371	−0.454 038	−2.118 534
100	−1.959 025	−0.042 260	−0.157 780	0.203 061	−0.485 308	−2.441 313
110	−2.468 758	−0.103 330	−0.130 322	0.266 094	−0.523 601	−2.959 917

TABLE V. Calculated values for f_{HA}^{1}, h_1, h_2, h_3, h_4, and f_{HA} for the $2P_{1/2}$ state.

Z	$f_{HA}^{1}(Z\alpha)$	$h_1(Z\alpha)$	$h_2(Z\alpha)$	$h_3(Z\alpha)$	$h_4(Z\alpha)$	$f_{HA}(Z\alpha)$
10	−0.988 462	0.069 822	−0.090 528	0.010 873	−0.089 114	−1.087 410
20	−1.003 798	0.070 915	−0.093 455	0.011 588	−0.091 679	−1.106 429
30	−1.030 396	0.072 663	−0.098 597	0.012 898	−0.096 104	−1.139 536
40	−1.069 984	0.074 996	−0.106 390	0.014 991	−0.102 678	−1.189 065
50	−1.125 389	0.077 806	−0.117 525	0.018 175	−0.111 863	−1.258 797
60	−1.201 096	0.080 907	−0.133 069	0.022 935	−0.124 357	−1.354 680
70	−1.304 319	0.083 957	−0.154 671	0.030 060	−0.141 212	−1.486 185
80	−1.447 140	0.086 292	−0.184 959	0.040 873	−0.164 034	−1.668 969
90	−1.651 160	0.086 568	−0.228 348	0.057 731	−0.195 383	−1.930 593
100	−1.959 025	0.081 847	−0.292 853	0.085 230	−0.239 612	−2.324 413
110	−2.468 758	0.064 809	−0.394 875	0.133 690	−0.304 933	−2.970 066

$$\frac{\gamma^4}{n^3}h_1(\gamma)=\tfrac{1}{10}\langle V\rangle+E_n\int_0^\infty dp\,p^4[\,|g_1(p)|^2+|g_2(p)|^2]Q_1(p^2)\,,$$

$$\frac{\gamma^4}{n^3}h_2(\gamma)=(\tfrac{1}{2}\ln 2-\tfrac{7}{20})\langle V\rangle+\int_0^\infty dp\,p^4[\,|g_1(p)|^2-|g_2(p)|^2]Q_2(p^2)\,,$$

$$\frac{\gamma^4}{n^3}h_3(\gamma)=\int_0^\infty dp\,p^4[g_1^*(p)(Vg)_1(p)+g_2^*(p)(Vg)_2(p)]Q_3(p^2)\,, \tag{3.6}$$

$$\frac{\gamma^4}{n^3}h_4(\gamma)=E_n^{-1}\int_0^\infty dp\,p^4[g_1^*(p)(Vg)_1(p)-g_2^*(p)(Vg)_2(p)]Q_4(p^2)\,.$$

The functions Q_i, $i=1,2,3,4$, are displayed in (I4.18) and (I4.19). The "radial" components of the momentum-space wave functions g_1, g_2, and the related functions $(Vg)_1$, $(Vg)_2$, are listed in Appendix A. The integrals in (3.6) were evaluated by 60-point Gaussian quadrature with the aid of a new variable of integration x defined by

$$p=(1-E_n^2)^{1/2}\frac{1-x^2}{x^2}\quad\text{in } h_1,h_2\,,$$

$$p=(1-E_n^2)^{1/2}\frac{1-x^3}{x^3}\quad\text{in } h_3,h_4\,. \tag{3.7}$$

The results are listed in Tables IV–VI as are the results for the total f_{HA}. The small-γ limits of the functions

TABLE VI. Calculated values for f_{HA}^{1}, h_1, h_2, h_3, h_4, and f_{HA} for the $2P_{3/2}$ state.

Z	$f_{HA}^{1}(Z\alpha)$	$h_1(Z\alpha)$	$h_2(Z\alpha)$	$h_3(Z\alpha)$	$h_4(Z\alpha)$	$f_{HA}(Z\alpha)$
10	−0.378 702	0.019 323	−0.087 988	0.010 742	−0.088 560	−0.525 185
20	−0.379 881	0.018 966	−0.088 361	0.011 023	−0.089 395	−0.527 649
30	−0.381 863	0.018 375	−0.088 978	0.011 483	−0.090 726	−0.531 709
40	−0.384 674	0.017 542	−0.089 829	0.012 124	−0.092 516	−0.537 353
50	−0.388 349	0.016 452	−0.090 904	0.012 948	−0.094 733	−0.544 586
60	−0.392 937	0.015 083	−0.092 188	0.013 960	−0.097 350	−0.553 431
70	−0.398 502	0.013 411	−0.093 663	0.015 168	−0.100 340	−0.563 927
80	−0.405 125	0.011 406	−0.095 309	0.016 577	−0.103 676	−0.576 127
90	−0.412 905	0.009 034	−0.097 100	0.018 192	−0.107 326	−0.590 104
100	−0.421 967	0.006 260	−0.099 005	0.020 019	−0.111 255	−0.605 948
110	−0.432 466	0.003 047	−0.100 989	0.022 059	−0.115 423	−0.623 773

$h_i(\gamma)$ are

$$h_1(0)=\frac{32}{105}\frac{1}{2l+1}-\frac{11}{84}\frac{1}{n}+\frac{1}{10}\frac{1}{\kappa(2l+1)}\ ,$$
$$h_2(0)=(2\ln 2-\tfrac{172}{105})\frac{1}{2l+1}+(\tfrac{23}{140}-\tfrac{1}{4}\ln 2)\frac{1}{n}+(\tfrac{1}{2}\ln 2-\tfrac{7}{20})\frac{1}{\kappa(2l+1)}\ , \tag{3.8}$$
$$h_3(0)=(\tfrac{31}{15}-3\ln 2)\left[\frac{1}{n}-\frac{4}{2l+1}\right],\quad h_4(0)=(4\ln 2-\tfrac{8}{3})\left[\frac{1}{n}-\frac{4}{2l+1}\right].$$

The small-γ limit for the total $f_{HA}(\gamma)$ is

$$f_{HA}(0)=(\tfrac{11}{10}-\ln 2)\frac{1}{n}+(\tfrac{16}{15}-2\ln 2)\frac{1}{2l+1}+(\tfrac{1}{2}\ln 2-\tfrac{1}{4})\frac{1}{\kappa(2l+1)}+(\tfrac{3}{2}\ln 2-\tfrac{9}{4})\frac{1}{|\kappa|}\ . \tag{3.9}$$

IV. THE HIGH-ENERGY REMAINDER ΔE_{HB}

The high-energy remainder is

$$\Delta E_{HB}=-\frac{i\alpha}{2\pi}\int_{C_H}dz\int_0^\infty dx_2x_2^2\int_0^\infty dx_1x_1^2\sum_\kappa\sum_{i,j=1}^{2}[f_i(x_2)G^{ij}_{B,\kappa}(x_2,x_1,z)f_j(x_1)A_\kappa(x_2,x_1)$$
$$-f_{\hat{i}}(x_2)G^{ij}_{B,\kappa}(x_2,x_1,z)f_{\hat{j}}(x_1)A^{ij}_\kappa(x_2,x_1)] \tag{4.1}$$

with $\hat{i},\hat{j}$ as in Eq. (2.1). In (4.1) the contour C_H extends from $-i\infty$ to 0 and from 0 to $i\infty$. In the regions $\mathrm{Im}(z)>0$ and $\mathrm{Im}(z)<0$, separate branches of the function b are specified by the definition

$$b=-i[(E_n-z)^2]^{1/2}\ ,\quad \mathrm{Re}(b)>0\ . \tag{4.2}$$

The function b enters the integrand of (4.1) via Eqs. (4.3) below. The functions f_i, $i=1,2$, are the components of the radial wave function as before, and the functions $G^{ij}_{B,\kappa}$ are defined in (I 5.5). Here, the functions A_κ and A^{ij}_κ are as defined in (I 5.8), with the explicit formulas (see also Ref. 14)

$$A_\kappa(x_2,x_1)=-\frac{b|\kappa|}{2\kappa\kappa_n}\sum_{l'}[(\kappa+\kappa_n)(\kappa+\kappa_n+1)-l'(l'+1)]$$
$$\times\langle l(\kappa)0l(\kappa_n)0\,|\,l(\kappa)l(\kappa_n)l'0\rangle^2 j_{l'}(ibx_<)h^{(1)}_{l'}(ibx_>)\ ,$$
$$A^{11}_\kappa(x_2,x_1)=-\frac{b|\kappa|}{2\kappa\kappa_n}\sum_{l'}[8\kappa\kappa_n+(\kappa-\kappa_n)(\kappa-\kappa_n+1)-l'(l'+1)]$$
$$\times\langle l(\kappa)0l(-\kappa_n)0\,|\,l(\kappa)l(-\kappa_n)l'0\rangle^2 j_{l'}(ibx_<)h^{(1)}_{l'}(ibx_>)\ ,$$
$$A^{12}_\kappa(x_2,x_1)=\frac{b|\kappa|}{2\kappa\kappa_n}\sum_{l'}[(\kappa-\kappa_n)(\kappa-\kappa_n-1)-l'(l'+1)] \tag{4.3}$$
$$\times\langle l(-\kappa)0l(\kappa_n)0\,|\,l(-\kappa)l(\kappa_n)l'0\rangle^2 j_{l'}(ibx_<)h^{(1)}_{l'}(ibx_>)\ ,$$
$$A^{21}_\kappa(x_2,x_1)=\frac{b|\kappa|}{2\kappa\kappa_n}\sum_{l'}[(\kappa-\kappa_n)(\kappa-\kappa_n+1)-l'(l'+1)]$$
$$\times\langle l(\kappa)0l(-\kappa_n)0\,|\,l(\kappa)l(-\kappa_n)l'0\rangle^2 j_{l'}(ibx_<)h^{(1)}_{l'}(ibx_>)\ ,$$
$$A^{22}_\kappa(x_2,x_1)=-\frac{b|\kappa|}{2\kappa\kappa_n}\sum_{l'}[8\kappa\kappa_n+(\kappa-\kappa_n)(\kappa-\kappa_n-1)-l'(l'+1)]$$
$$\times\langle l(-\kappa)0l(\kappa_n)0\,|\,l(-\kappa)l(\kappa_n)l'0\rangle^2 j_{l'}(ibx_<)h^{(1)}_{l'}(ibx_>)\ .$$

In (4.3), j is the spherical Bessel function, $h^{(1)}$ is the spherical Hankel function of the first kind, $x_<=\min(x_1,x_2)$, $x_>=\max(x_1,x_2)$, $\langle\ \rangle$ denotes vector addition coefficients in the notation of Edmonds,[20] and l' is summed over non-negative integers for which the coefficients are nonzero.

The integral over z in (4.1) is transformed according to

$$-\frac{i}{2}\int_{C_H} dz\, W(z,b)=\mathrm{Re}\int_0^\infty du\, W(iu,u+iE_n)\ , \tag{4.4}$$

valid when $W^*(iu,u+iE_n)=W(-iu,u-iE_n)$ as in Eq. (4.1). In terms of the new variables r and y defined in (2.5), $t=(u^2+1)^{1/2}-u$, and the function f_{HB} defined by

$$\Delta E_{HB}=\frac{\alpha}{\pi}\frac{\gamma^4}{n^3}f_{HB}(\gamma) \tag{4.5}$$

we have

$$f_{HB}(\gamma)=\int_0^1 dt\int_0^\infty dy\int_0^1 dr\, S(r,y,t,\gamma)\ , \tag{4.6}$$

where

$$S(r,y,t,\gamma)=\sum_{\kappa=1}^{\infty} T_\kappa(r,y,t,\gamma) \tag{4.7}$$

and

$$T_\kappa(r,y,t,\gamma)=\frac{n^3r^2y^5}{\gamma^4a^6}(1+t^{-2})\sum_{\substack{\text{signs}\\ \text{of }\kappa}}\sum_{i,j=1}^{2}\mathrm{Re}[f_i(ry/a)G^{ij}_{B,\kappa}(ry/a,y/a,z)f_j(y/a)A_\kappa(ry/a,y/a)$$
$$-f_{\hat{i}}(ry/a)G^{ij}_{B,\kappa}(ry/a,y/a,z)f_{\hat{j}}(r/a)A^{ij}_\kappa(ry/a,y/a)]\ . \tag{4.8}$$

Individual terms in the sum in (4.8) are calculated as described in Ref. 2. The sum over κ in (4.7) is terminated when κ is larger than $3(t+t^{-1})y/(4a)+3$ and (see Ref. 2)

$$\max(|T_\kappa|,|T_{\kappa-1}|,|T_{\kappa-2}|,|T_{\kappa-3}|,|T_{\kappa-4}|)<10^{-4}(1-r^2)\ . \tag{4.9}$$

The validity of this procedure was checked by reducing the error estimate (10^{-4}) in (4.9) by two orders of magnitude in certain evaluations of f_{HB}, and by the test calculation described in Appendix E. As another check, in the evaluation of the $2P_{3/2}$ level shift, the estimated remainder from the sum over κ was integrated over r, y, and t, and found to give a negligible contribution to f_{HB}.

Numerical integration of $S(r,y,t,\gamma)$ is carried out by applying a Gauss-Legendre formula for integrals over the interval (0,1) and a Gauss-Laguerre formula for the integral over the interval $(0,\infty)$, with new variables of integration displayed below. The integral over r in (4.6) is evaluated by

$$S_1(y,t,\gamma)=\int_0^1 dx\, 2xS(x^2,y,t,\gamma),\quad 0\le q\le 1$$
$$S_1(y,t,\gamma)=\int_0^1 dx\, S(x,y,t,\gamma),\quad 1<q\le 12 \tag{4.10}$$

$$S_1(y,t,\gamma)=\int_0^1 dx\,\frac{12}{q}S(1-12x/q,y,t,\gamma)$$
$$+\epsilon,\quad q>12$$

where

$$q=y/(ta)-y/2 \tag{4.11}$$

and $N=6$ in each case. The residual ϵ is discussed in Ref. 2. The integration over y is done in two parts:

$$S_{21}(t,\gamma)=\int_0^1 dx\, 8xS_1(4x^2,t,\gamma),\quad N=14 \tag{4.12a}$$

$$S_{22}(t,\gamma)=\int_0^\infty dx\, S_1(4+x,t,\gamma),\quad N=3\ . \tag{4.12b}$$

And finally

$$S_{3i}(\gamma)=\int_0^1 dx\, S_{2i}(t,\gamma)\ ,\quad i=1,2 \tag{4.13}$$

with $N=4$.

Calculated results for S_{31} and S_{32} appear in Table VII. As in Sec. II, each integral was evaluated with $N+I$ integration points, where N is the number associated with each integral in (4.10), (4.12), and (4.13) and the value of I is listed with the corresponding result in the table. Results for f_{HB}

$$f_{HB}(\gamma)=S_{31}(\gamma)+S_{32}(\gamma) \tag{4.14}$$

appear in Table VIII. The number in parentheses in that table is the estimated uncertainty in the last figure, based on the apparent stability of the values as the number of integration points is varied. This method of calculation and uncertainty estimation has been tested as described in Appendix E.

The values for the function $f_{HB}(\gamma)$ are compared to the exact values of $f_{HB}(0)$ in Fig. 3. The values of $f_{HB}(0)$ follow from (I 5.11),

$$f_{HB}(0)=\frac{1}{(2l+1)}\left[\left(\tfrac{17}{18}-\tfrac{4}{3}\ln 2\right)\delta_{l0}+\left(\tfrac{3}{2}-2\ln 2\right)\frac{1}{\kappa}+\left(\tfrac{5}{6}-\ln 2\right)\frac{n-2l-1}{n}\right]. \tag{4.15}$$

There is apparent consistency between the calculated values and the values at $\gamma=0$.

The calculated values for the function f_{HB} for

TABLE VII. Calculated values for the functions S_{31} and S_{32}.

		$S_{31}(Z\alpha)$			$S_{32}(Z\alpha)$		
Z	I	$2S_{1/2}$	$2P_{1/2}$	$2P_{3/2}$	$2S_{1/2}$	$2P_{1/2}$	$2P_{3/2}$
10	−1	0.064 913	0.046 609		−0.026 039	−0.025 263	
	0	0.066 534	0.042 865		−0.027 381	−0.026 586	
	1	0.065 356	0.042 534		−0.027 355	−0.026 630	
20	0	0.139 546	0.046 464	−0.029 374			
	1	0.139 821	0.046 141	−0.029 060	−0.027 634	−0.027 101	−0.011 569
30	−1	0.224 700	0.055 333	−0.023 011	−0.026 357	−0.025 862	−0.009 968
	0	0.219 352	0.052 740	−0.026 665	−0.027 768	−0.027 336	−0.011 744
	1	0.219 508	0.052 557	−0.026 373	−0.027 808	−0.027 433	−0.011 770
40	1	0.304 853	0.062 910	−0.022 858	−0.027 876	−0.027 627	−0.011 829
50	−1	0.404 218	0.080 364	−0.016 462	−0.026 165	−0.025 882	−0.009 714
	0	0.399 568	0.078 813	−0.018 954	−0.027 766	−0.027 599	−0.011 692
	1	0.399 594	0.078 942	−0.018 579	−0.027 830	−0.027 677	−0.011 738
60	1	0.508 264	0.103 414	−0.013 632	−0.027 640	−0.027 572	−0.011 495
70	−1	0.642 345	0.142 460	−0.006 218	−0.026 036	−0.026 172	−0.009 894
	0	0.638 193	0.140 732	−0.008 475	−0.027 451	−0.027 345	−0.011 184
	1	0.637 546	0.140 832	−0.008 148	−0.027 347	−0.027 268	−0.011 102
80	1	0.798 127	0.199 069	−0.002 299	−0.027 069	−0.026 796	−0.010 585
90	−1	1.013 412	0.296 042	0.005 486	−0.026 031	−0.025 464	−0.009 277
	0	1.009 604	0.293 068	0.003 427	−0.026 915	−0.026 490	−0.010 110
	1	1.007 993	0.292 834	0.003 642	−0.026 680	−0.026 327	−0.009 966
100	1	1.300 956	0.452 056	0.009 169	−0.025 605	−0.026 078	−0.009 234
110	−1	1.752 620	0.756 189	0.014 959	−0.021 687	−0.025 488	−0.007 931
	0	1.753 713	0.748 067	0.013 120	−0.023 047	−0.026 240	−0.008 488
	1	1.752 211	0.747 028	0.013 280	−0.022 875	−0.026 051	−0.008 315

TABLE VIII. Values and estimated uncertainties for f_{HB}.

Z	$f_{HB}(Z\alpha)$ $2S_{1/2}$	$2P_{1/2}$	$2P_{3/2}$
10	0.038(2)	0.0159(4)	
20	0.1122(4)	0.0190(4)	−0.0406(4)
30	0.1917(3)	0.0251(4)	−0.0381(4)
40	0.2770(3)	0.0353(4)	−0.0347(4)
50	0.3718(2)	0.0513(3)	−0.0303(4)
60	0.4806(4)	0.0758(3)	−0.0251(4)
70	0.6102(8)	0.1136(3)	−0.0193(4)
80	0.771(2)	0.1723(3)	−0.0129(4)
90	0.981(3)	0.2665(3)	−0.0063(4)
100	1.275(3)	0.426(1)	−0.0001(4)
110	1.729(3)	0.721(2)	0.0050(4)

the $2P_{3/2}$ state appear to be consistent with the functional form $A+B\gamma^2$ for small Z. Interpolation with such a function between $Z=0$ and $Z=20$ yields $f_{HB}(10\alpha)=-0.0419(4)$ for the $2P_{3/2}$ state.

V. CONCLUSION

The total self-energy level shift is expressed in terms of the function $F_n(Z\alpha)$ defined by

$$\Delta E_n=\frac{\alpha}{\pi}\frac{(Z\alpha)^4}{n^3}F_n(Z\alpha)m_ec^2\ . \tag{5.1}$$

The function F is the sum

$$F_n(Z\alpha)=f_L(Z\alpha)+f_{HA}(Z\alpha)+f_{HB}(Z\alpha)\ , \tag{5.2}$$

where the separate contributions on the right-hand side appear in Eqs. (2.14), (3.2), and (4.14). Results of this calculation of F appear in Table IX.

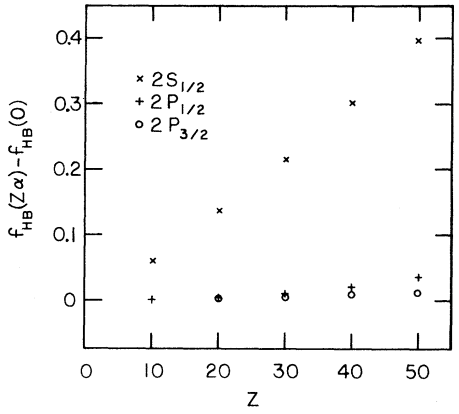

FIG. 3. Calculated values for the difference $f_{HB}(\gamma)-f_{HB}(0)$.

The function F for the $2S_{1/2}$ state is qualitatively similar to the corresponding function for the $1S_{1/2}$ state.[2] The difference between the values of the function F for the $2P_{1/2}$ and $2P_{3/2}$ states, i.e., the radiative correction to the fine structure changes sign near $Z=90$ due to the rapid increase of F for the $2P_{1/2}$ state.

ACKNOWLEDGMENTS

Research was supported in part by the National Science Foundation, Grant No. PHY80-26549. Primary support for this work was provided by the Division of Chemical Sciences, Office of Basic Energy Sciences, U.S. Department of Energy, while the author was at Lawrence Berkeley Laboratory.

APPENDIX A

This appendix lists wave functions and related functions for the $n=2$ Dirac Coulomb states.

TABLE IX. Results of the self-energy calculation.

Z	$F(Z\alpha)$ $2S_{1/2}$	$2P_{1/2}$	$2P_{3/2}$
10	4.893(2)	−0.1145(4)	0.1303(4)
20	3.5063(4)	−0.0922(4)	0.1436(4)
30	2.8391(3)	−0.0641(4)	0.1604(4)
40	2.4550(3)	−0.0308(4)	0.1794(4)
50	2.2244(2)	0.0082(3)	0.1999(4)
60	2.0948(4)	0.0549(3)	0.2215(4)
70	2.0435(8)	0.1129(3)	0.2440(4)
80	2.065(2)	0.1884(3)	0.2671(4)
90	2.169(3)	0.2934(3)	0.2906(4)
100	2.387(3)	0.453(1)	0.3141(4)
110	2.798(3)	0.725(2)	0.3367(4)

In the notation[21]

$$\psi_n(\vec{x})=\begin{bmatrix} f_1(x)\chi^{\mu}_{\kappa}(\hat{x}) \\ if_2(x)\chi^{\mu}_{-\kappa}(\hat{x}) \end{bmatrix} \tag{A1}$$

the radial wave functions are for the $2S_{1/2}$ state:

$$\begin{aligned} f_1(x)&=N_1^{1/2}(1+E)^{1/2}[E(2E-1)-\gamma x/2E]x^{-\delta}e^{-\gamma x/2E}\,, \\ f_2(x)&=-N_1^{1/2}(1-E)^{1/2}[(E+1)(2E-1)-\gamma x/2E]x^{-\delta}e^{-\gamma x/2E}\,; \end{aligned} \tag{A2a}$$

$2P_{1/2}$ state:

$$\begin{aligned} f_1(x)&=N_2^{1/2}(1+E)^{1/2}[(E-1)(2E+1)-\gamma x/2E]x^{-\delta}e^{-\gamma x/2E}\,, \\ f_2(x)&=-N_2^{1/2}(1-E)^{1/2}[E(2E+1)-\gamma x/2E]x^{-\delta}e^{-\gamma x/2E}\,; \end{aligned} \tag{A2b}$$

$2P_{3/2}$ state:

$$f_1(x)=N_3^{1/2}(1+E')^{1/2}x^{1-\delta'}e^{-\gamma x/2}\,,\quad f_2(x)=-N_3^{1/2}(1-E')^{1/2}x^{1-\delta'}e^{-\gamma x/2}\,, \tag{A2c}$$

where

$$\begin{aligned} &\gamma=Z\alpha\,,\quad \delta=1-(1-\gamma^2)^{1/2}\,,\quad E=(1-\delta/2)^{1/2}\,,\quad \delta'=2-(4-\gamma^2)^{1/2}\,,\quad E'=1-\delta'/2\,, \\ &N_1=(\gamma/E)^{3-2\delta}/[E(2E-1)2\Gamma(3-2\delta)],\quad N_2=(\gamma/E)^{3-2\delta}/[E(2E+1)2\Gamma(3-2\delta)]\,, \\ &N_3=\gamma^{5-2\delta'}[2\Gamma(5-2\delta')]\,. \end{aligned} \tag{A3}$$

The momentum-space wave functions, defined by

$$\phi_n(\vec{p})=(2\pi)^{-3/2}\int d^3x\, e^{-i\vec{p}\cdot\vec{x}}\psi_n(\vec{x})=\begin{bmatrix} g_1(p)\chi^{\mu}_{k}(\hat{p}) \\ g_2(p)\chi^{\mu}_{-\kappa}(\hat{p}) \end{bmatrix} \tag{A4}$$

and the functions defined by

$$(V\phi_n)(\vec{p})=(2\pi)^{-3/2}\int d^3x\, e^{-i\vec{p}\cdot\vec{x}}V(\vec{x})\psi_n(\vec{x})=\begin{bmatrix} (Vg)_1(p)\chi^{\mu}_{\kappa}(\hat{p}) \\ (Vg)_2(p)\chi^{\mu}_{-\kappa}(\hat{p}) \end{bmatrix} \tag{A5}$$

are for the $2S_{1/2}$ state:

$$\begin{aligned} &g_1(p)=M_1^{1/2}(1+E)^{1/2}[E(2E-1)C_2-C_3]\,,\quad g_2(p)=-M_1^{1/2}(1-E)^{1/2}[(E+1)(2E-1)D_2-D_3]\,, \\ &(Vg)_1(p)=-\frac{\gamma^2}{2E}M_1^{1/2}(1+E)^{1/2}[E(2E-1)C_1-C_2]\,, \\ &(Vg)_2(p)=\frac{\gamma^2}{2E}M_1^{1/2}(1-E)^{1/2}[(E+1)(2E-1)D_1-D_2]\,; \end{aligned} \tag{A6a}$$

$2P_{1/2}$ state:

$$\begin{aligned} &g_1(p)=-iM_2^{1/2}(1+E)^{1/2}[(E-1)(2E+1)D_2-D_3]\,,\quad g_2(p)=-iM_2^{1/2}(1-E)^{1/2}[E(2E+1)C_2-C_3]\,, \\ &(Vg)_1(p)=i\frac{\gamma^2}{2E}M_2^{1/2}(1+E)^{1/2}[(E-1)(2E+1)D_1-D_2]\,, \\ &(Vg)_2(p)=i\frac{\gamma^2}{2E}M_2^{1/2}(1-E)^{1/2}[E(2E+1)C_1-C_2]\,; \end{aligned} \tag{A6b}$$

$2P_{3/2}$ state:

$$\begin{aligned} &g_1(p)=-iM_3^{1/2}(1+E')^{1/2}(D_3')\,,\quad g_2(p)=iM_3^{1/2}(1-E')^{1/2}(3D_2'/q'-C_3')\,, \\ &(Vg)_1(p)=i\frac{\gamma^2}{2}M_3^{1/2}(1+E')^{1/2}(D_2')\,,\quad (Vg)_2(p)=-i\frac{\gamma^2}{2}M_3^{1/2}(1-E')^{1/2}(3D_1'/q'-C_2')\,. \end{aligned} \tag{A6c}$$

In Eqs. (A6a)–(A6c)

$$q=2Ep/\gamma,\quad q'=2p/\gamma\ ,$$

$$C_m=\Gamma(m-\delta)\frac{\sin[(m-\delta)\tan^{-1}q]}{q(1+q^2)^{(m-\delta)/2}}\ ,\quad m=1,2,\ldots$$

$$D_m=\frac{C_{m-1}}{q}-\Gamma(m-\delta)\frac{\cos[(m-\delta)\tan^{-1}q]}{q(1+q^2)^{(m-\delta)/2}}\ ,\quad m=1,2,\ldots \tag{A7}$$

$$M_1=\frac{2^{6-2\delta}E^2}{\pi\gamma^3(2E-1)\Gamma(3-2\delta)}\ ,\quad M_2=\frac{2^{6-2\delta}E^2}{\pi\gamma^3(2E+1)\Gamma(3-2\delta)}\ ,\quad M_3=\frac{2^{8-2\delta'}}{\pi\gamma^3\Gamma(5-2\delta')}$$

and C'_m,D'_m are obtained by replacing q and δ by q' and δ' in C_m,D_m.

The transforms of the square of the Coulomb wave functions, defined by

$$L_n(u)=\int d^3x\,|\psi_n(\vec{x})|^2\frac{e^{-ux}}{x}=\int_0^\infty dx\,xe^{-ux}[f_1^2(x)+f_2^2(x)] \tag{A8}$$

are for the $1S_{1/2}$ state:

$$L(u)=\frac{\gamma}{1-\delta}\left[1+\frac{u}{(2\gamma)}\right]^{2\delta-2}\ ; \tag{A9a}$$

$2S_{1/2}$ state:

$$L(u)=\frac{\gamma}{4E(1-\delta)}[1+4E(1-E^2)u/\gamma+E(1+E)(2E-1)(u/\gamma)^2](1+uE/\gamma)^{2\delta-4}\ ; \tag{A9b}$$

$2P_{1/2}$ state:

$$L(u)=\frac{\gamma}{4E(1-\delta)}[1+4E(1-E^2)u/\gamma+E(1-E)(2E+1)(u/\gamma)^2](1+uE/\gamma)^{2\delta-4}\ ; \tag{A9c}$$

$2P_{3/2}$ state:

$$L(u)=\frac{\gamma}{2(2-\delta')}(1+u/\gamma)^{2\delta'-4}\ . \tag{A9d}$$

APPENDIX B

In the numerical evaluation of the radial Green's functions for the low-energy part, the domain of one of the parameters of the Whittaker functions is larger for the $n=2$ states calculation than it is for the $n=1$ state calculation. The necessary modifications of the method (in Ref. 2) of evaluation of these functions is summarized here.

The domain of the parameters for $M_{\alpha,\beta}(x)$ and $W_{\alpha,\beta}(x)$ is here within the limits $-\frac{1}{2}<\alpha<\frac{5}{2}$, $0<\beta<500$, $0<x<500$, $\beta+\frac{1}{2}-\alpha>-2$. The effect of the extended domain of the parameters is to modify the conditions governing the truncation of the summations. In the present evaluation, Eq. (II D3) is replaced by

$$\left|\sum_{n=N+1}^{\infty}T(n)\right|<\frac{N+2}{N+2-x}\,|T(N+1)|$$

$$\text{for } N+2>x \text{ and } N\geq 0\ . \tag{B1}$$

The condition on Eq. (II D11) is replaced by $N+2>\max(2\beta+\frac{3}{2},\theta x)$ with θ as given by (II D12).

APPENDIX C

The method of evaluation of principal value integrals, described in Sec. II, is examined in more detail in this appendix. Consider a function $f(x)$ which is analytic on the interval $(-1,1)$ except for a pole at $x=0$. We may write

$$f(x)=\frac{R}{x}+g(x)\ , \tag{C1}$$

where R is the residue of the pole of $f(x)$, and $g(x)$ is analytic on the interval $(-1,1)$. Then the principal value integral of $f(x)$ is given by

$$K=P\int_{-1}^{1}dx\,f(x)=\int_{-1}^{1}dx\,g(x)\ . \tag{C2}$$

The integral in (C2) is numerically evaluated by

simply applying an N-point Gaussian quadrature formula, with the provision that N is even. In particular,

$$K \simeq \sum_{i=1}^{N} w_i f(x_i) = \sum_{i=1}^{N} w_i g(x_i) \ , \quad N \text{ even} \tag{C3}$$

where w_i and x_i are the weights and evaluation points of the quadrature formula. The validity of this method follows from the fact that the pole term vanishes identically in (C3) because of the symmetry of the weights and evaluation points in the quadrature formula, i.e., $w_i = w_{N+1-i}$ and $x_i = -x_{N+1-i}$, $i = 1,2,\ldots,N$. Hence, the theoretical accuracy of this method is the same as that of the quadrature formula applied to the analytic function $g(x)$. In any numerical calculation, there will be an additional error associated with the fact that the function $f(x)$ is evaluated only approximately. This numerical error may be enhanced due to cancellations between the values of $f(x)$ at integration points near the pole at $x=0$. In this calculation, such numerical error is negligible.

APPENDIX D

This appendix describes the residue test of the numerical evaluation program for the low-energy part. The imaginary part of the lowest-order self-energy of a state is proportional to the sum of all one-photon decay rates to states of lower energy,

$$\mathrm{Im}(\Delta E_n) = -\tfrac{1}{2} \sum_m A(n \to m), \quad E_m < E_n \ . \tag{D1}$$

We also know from inspection of (I 3.8) that

$$\mathrm{Im}(\Delta E_n) = \pi \sum_m R_m, \quad E_m < E_n \tag{D2}$$

where R_m is the residue of the pole of the integrand at E_m in the integral over k in Eq. (I 3.8). Hence, identifying the transition rate to a state m with the residue of the pole at E_m,

$$A(n \to m) = -2\pi R_m \ , \tag{D3}$$

TABLE X. $M1$ decay rate $A(2S_{1/2} \to 1S_{1/2})$.

Z	I	$A/(2\alpha)$
50	0	$2.500\,480 \times 10^{-8}$
	1	$2.498\,047 \times 10^{-8}$
	exact	$2.497\,968 \times 10^{-8}$
100	0	$4.544\,803 \times 10^{-5}$
	exact	$4.544\,668 \times 10^{-5}$

TABLE XI. $E1$ decay rate $A(2P_{1/2} \to 1S_{1/2})$.

Z	I	$A/(2\alpha)$
50	0	$3.512\,683\,0 \times 10^{-4}$
	1	$3.512\,682\,8 \times 10^{-4}$
	exact	$3.512\,682\,7 \times 10^{-4}$
100	0	$5.862\,496\,1 \times 10^{-3}$
	exact	$5.862\,496\,1 \times 10^{-3}$

or

$$A(n \to m) = -2\alpha \lim_{t \to t_m} [(t - t_m) S_2(t,\gamma)] \ , \tag{D4}$$

where t_m is the location of the pole, in terms of the variable t defined in (2.5), corresponding to state m. Numerical values for the limit in (D4) are obtained by evaluating the function $(t-t_m)S_2(t,\gamma)$ at the points $t = t_m - 2\epsilon$, $t_m - \epsilon$, $t_m + \epsilon$, $t_m + 2\epsilon$ and applying a third-degree polynomial interpolation to find the value at $t = t_m$. The value employed for ϵ was $\epsilon = 10^{-5}$, except in one transition where $\epsilon = 10^{-4}$ was employed. This result for the decay rate is compared to an independent exact numerical calculation based on standard relativistic formulas for the one-photon decay rates. The results are shown in Tables X–XIII (in units of $m_e c^2/\hbar$). In those tables, the value for the integration index I, discussed in Sec. II, is listed with the corresponding integrated and interpolated values. The interpolated decay rates all have absolute errors less than 3×10^{-9} (not including the factor α) and show good convergence to the exact values as the number of integration points is increased.

APPENDIX E

This appendix describes a procedure employed to check the high-energy parts of the calculation. The test indicates that computational errors are unlikely, and shows that the degree of stability of the calculated values for the high-energy remainder, as the

TABLE XII. $E1, M2$ decay rate $A(2P_{3/2} \to 1S_{1/2})$, $\epsilon = -4$.

Z	I	$A/(2\alpha)$
50	0	$3.348\,067\,7 \times 10^{-4}$
	2	$3.348\,068\,1 \times 10^{-4}$
	exact	$3.348\,068\,1 \times 10^{-4}$
100	0	$4.710\,936\,0 \times 10^{-3}$
	2	$4.710\,936\,4 \times 10^{-3}$
	exact	$4.710\,936\,4 \times 10^{-3}$

number of integration points is varied, is a valid measure of the accuracy of the values.

The procedure is to calculate a test energy-level shift ΔE_T both by the method employed to calculate ΔE_{HA} (method A: Sec. III) and by the method employed to calculate ΔE_{HB} (method B: Sec. IV), and then compare the results. The favorable outcome is taken as evidence for the validity of the methods and programs employed in both cases. The test energy-level shift is

TABLE XIII. $E1, M2, M1, E2$ decay rate $A(2P_{3/2} \rightarrow 2S_{1/2}, 2P_{1/2})$.

Z	I	$A/(2\alpha)$
50	0	$9.502\,578 \times 10^{-9}$
	2	$9.496\,500 \times 10^{-9}$
	exact	$9.496\,625 \times 10^{-9}$
100	0	$2.155\,226 \times 10^{-5}$
	2	$2.155\,223 \times 10^{-5}$
	exact	$2.155\,222 \times 10^{-5}$

$$\Delta E_T = -\frac{i\alpha}{2\pi} \int d^3x_2 \int d^3x_1 \psi_n^\dagger(\vec{x}_2)\alpha_\mu \int_{C_H} dz\, G_T(\vec{x}_2, \vec{x}_1, z)\alpha^\mu \psi_n(\vec{x}_1) \frac{1}{\rho} e^{-b\rho}\,, \tag{E1}$$

where $\rho = |\vec{x}_2 - \vec{x}_1|$, G_T is the kernel corresponding to the operator

$$G_T(z) = V \frac{1}{(H_0 - z)^3} V\,, \tag{E2}$$

V is the Coulomb potential, and H_0 is the free Dirac Hamiltonian $H_0 = \vec{\alpha}\cdot\vec{p} + \beta$. This operator is analytically similar to G_B of Sec. IV, and is sufficiently simple that method A may be applied to calculate ΔE_T.

For method A, we find

$$\Delta E_T = \frac{\alpha}{\pi} \langle V[T_1(p^2) + \beta T_2(p^2) + \vec{\alpha}\cdot\vec{p}\, T_3(p^2)]V \rangle\,, \tag{E3}$$

where

$$T_1(p^2) = -\tfrac{1}{2}\,\mathrm{Im} \int_0^1 dt \left[2(1+4t^2+t^4) \frac{1-t^2}{(1+t^2)^2} \frac{1}{t^2p^2 + (1-iE_nt)^2} - \frac{(1-t^2)^3}{(1+t^2)} \frac{1-iE_nt}{[t^2p^2 + (1-iE_nt)^2]^2} \right],$$

$$T_2(p^2) = \mathrm{Re} \int_0^1 dt \left[\frac{8t^3}{(1+t^2)^2} \frac{1}{t^2p^2 + (1-iE_nt)^2} - \frac{2t(1-t^2)^2}{(1+t^2)} \frac{1-iE_nt}{[t^2p^2 + (1-iE_nt)^2]^2} \right], \tag{E4}$$

$$T_3(p^2) = \tfrac{1}{2}\,\mathrm{Re} \int_0^1 dt \left[\frac{1+t^2}{t^2p^2} \left[\frac{1}{2p} \{ \tan^{-1}[(E_n+p)t] - \tan^{-1}[(E_n-p)t] \} - \frac{t}{1-iE_nt} \right] + \frac{t(1+t^2)}{1-iE_nt} \frac{1}{t^2p^2 + (1-iE_nt)^2} - \frac{t(1-t^2)^2}{[t^2p^2 + (1-iE_nt)^2]^2} \right].$$

TABLE XIV. Results of the test calculation.

Z	Method	I	$F_T(2S_{1/2})$	$F_T(2P_{1/2})$	$F_T(2P_{3/2})$
20	B	0	−0.3195	−0.1448	−0.1381
20	A		−0.3189	−0.1449	−0.1382
60	B	0	−0.1661	−0.1837	−0.1243
60	B	1	−0.1663	−0.1835	−0.1242
60	A		−0.1661	−0.1834	−0.1241
100	B	0	0.0652	−0.2610	−0.0962
100	B	1	0.0664	−0.2608	−0.0959
100	A		0.0675	−0.2607	−0.0959

The integrals in (E4) are evaluated numerically, and the matrix elements in (E3) are evaluated as in method A.

To apply method B, the function $G_T(\vec{x}_2,\vec{x}_1,z)$ is expanded in spin-angle eigenfunctions in analogy with formula (I A14). The radial functions in this case are for $x_1>x_2$ [the symmetry conditions (IA18) apply here]

$$
\begin{aligned}
G^{11}_{T,\kappa}(x_2,x_1,z)&=-\frac{\gamma^2}{2x_2x_1}\left[(z+1)\frac{z^2}{c}[(x_2^2+x_1^2)j_+h_+-2x_2x_1j_-h_-]\right.\\
&\quad\left.+\frac{1+2z+2\kappa z^2}{1-z}\left[\frac{2\kappa+1}{c}j_+h_+-i\frac{\kappa}{|\kappa|}(x_2j_-h_++x_1j_+h_-)\right]\right],\\
G^{12}_{T,\kappa}(x_2,x_1,z)&=\frac{\gamma^2}{2x_2x_1}\left[\frac{1}{c}[(2\kappa z^2-1)x_2j_-h_-+(2\kappa z^2+1)x_1j_+h_+]\right.\\
&\quad\left.-i\frac{\kappa}{|\kappa|}z^2[(x_2^2+x_1^2)j_+h_-+2x_2x_1j_-h_+]\right],\\
G^{21}_{T,\kappa}(x_2,x_1,z)&=\frac{\gamma^2}{2x_2x_1}\left[\frac{1}{c}[(2\kappa z^2+1)x_2j_+h_++(2\kappa z^2-1)x_1j_-h_-]\right.\\
&\quad\left.-i\frac{\kappa}{|\kappa|}z^2[(x_2^2+x_1^2)j_-h_++2x_2x_1j_+h_-]\right],\\
G^{22}_{T,\kappa}(x_2,x_1,z)&=-\frac{\gamma^2}{2x_2x_1}\left[(z-1)\frac{z^2}{c}[(x_2^2+x_1^2)j_-h_--2x_2x_1j_+h_+]\right.\\
&\quad\left.+\frac{1-2z-2\kappa z^2}{1+z}\left[\frac{2\kappa-1}{c}j_-h_--i\frac{\kappa}{|\kappa|}(x_2j_+h_-+x_1j_-h_+)\right]\right],
\end{aligned}
\tag{E5}
$$

where $j_\pm=j_{|\kappa\pm1/2|-1/2}(icx_2)$ and $h_\pm=h^{(1)}_{|\kappa\pm1/2|-1/2}(icx_1)$, $c=(1-z^2)^{1/2}$, $\mathrm{Re}(c)>0$. Method B is then applied with the replacement $G^{ij}_{B,\kappa}\to G^{ij}_{T,\kappa}$.

The results of both methods of calculation appear in Table XIV. The results of method A should be exact to the number of figures shown. For method B, the parameter I in Table XIV is defined as in Sec. IV. The results are written in terms of the function f_T defined by

$$\Delta E_T=\frac{\alpha}{\pi}\frac{\gamma^4}{n^3}f_T(\gamma)\ . \tag{E6}$$

The agreement between the two methods is consistent with the estimated uncertainties listed in Table VIII.

APPENDIX F

Wichmann and Kroll have shown that the effect of vacuum polarization on Coulomb energy levels is dominated by the Uehling potential over a wide range of Z.[4] As an aid in evaluating radiative level shifts in a Coulomb field, calculated values for the Uehling potential shifts are give here.

The Uehling potential $U(x)$ in a Coulomb field is[5,6]

$$U(x)=-\frac{\alpha}{\pi}\gamma\int_1^\infty dt\,(t^2-1)^{1/2}\times\left[\frac{2}{3t^2}+\frac{1}{3t^4}\right]\frac{e^{-2tx}}{x}\ . \tag{F1}$$

Hence, the energy-level shift is

$$\Delta E_U=\int d^3x\,|\psi_n(\vec{x})|^2U(x)\ , \tag{F2}$$

or

$$\Delta E_U=-\frac{\alpha}{\pi}\gamma\int_1^\infty dt\,(t^2-1)^{1/2}\left[\frac{2}{3t^2}+\frac{1}{3t^4}\right]L_n(2t)\ , \tag{F3}$$

where

$$L_n(u)=\int d^3x\,|\psi_n(\vec{x})|^2\frac{e^{-ux}}{x}\ . \tag{F4}$$

The transforms of the square of the wave function L_n are listed in Appendix A. In terms of the new variable $x=1-(1-t^{-2})^{1/2}$ and the function H_U defined by

$$\Delta E_U=\frac{\alpha}{\pi}\frac{\gamma^4}{n^3}H_U(\gamma)m_ec^2 \tag{F5}$$

TABLE XV. Calculated values for the function H_U.

	$H_U(Z\alpha)$			
Z	$1S_{1/2}$	$2S_{1/2}$	$2P_{1/2}$	$2P_{3/2}$
10	−0.249 449	−0.250 399	−0.000 335	−0.000 069
20	−0.240 914	−0.244 587	−0.001 370	−0.000 255
30	−0.238 684	−0.246 936	−0.003 257	−0.000 536
40	−0.242 087	−0.257 197	−0.006 323	−0.000 902
50	−0.251 334	−0.276 418	−0.011 150	−0.001 349
60	−0.267 463	−0.307 130	−0.018 773	−0.001 876
70	−0.292 650	−0.354 174	−0.031 087	−0.002 490
80	−0.331 025	−0.426 679	−0.051 786	−0.003 199
90	−0.390 672	−0.542 896	−0.088 728	−0.004 019
100	−0.489 026	−0.743 531	−0.160 837	−0.004 969
110	−0.670 610	−1.136 909	−0.323 108	−0.006 075

we have

$$H_U(\gamma)=-\frac{1}{3}\left[\frac{n}{\gamma}\right]^3\int_0^1 dx\,(1-x)^2\frac{2+2x-x^2}{2x-x^2}\times L_n[2/(2x-x^2)^{1/2}]\,. \tag{F6}$$

To reduce the effect of the singularity at $x=0$ on the numerical accuracy, a new variable of integration s, where $x=s^6$, is employed in the numerical evaluation of (F6). Integration over s by 20-point Gauss-Legendre quadrature yields the results listed in Table XV.[22]

[1]P. J. Mohr, Ann. Phys. (N.Y.) 88, 26 (1974).
[2]P. J. Mohr, Ann. Phys. (N.Y.) 88, 52 (1974).
[3]P. J. Mohr, Phys. Rev. Lett. 34, 1050 (1975).
[4]E. H. Wichmann and N. M. Kroll, Phys. Rev. 101, 843 (1956).
[5]E. A. Uehling, Phys. Rev. 48, 55 (1935).
[6]R. Serber, Phys. Rev. 48, 49 (1935).
[7]J. D. Garcia and J. E. Mack, J. Opt. Soc. Am. 55, 654 (1965).
[8]P. J. Mohr, in *Beam-Foil Spectroscopy,* edited by I. A. Sellin and D. J. Pegg (Plenum, New York, 1976), p. 89.
[9]G. W. Erickson, J. Phys. Chem. Ref. Data 6, 831 (1977).
[10]O. R. Wood, II, C. K. N. Patel, D. E. Murnick, E. T. Nelson, M. Leventhal, H. W. Kugel, and Y. Niv, Phys. Rev. Lett. 48, 398 (1982).
[11]H. Gould and R. Marrus, Phys. Rev. Lett. 41, 1457 (1978).
[12]P. J. Mohr, in Proceedings of the Workshop on Foundations of the Relativistic Theory of Atomic Structure, Argonne National Laboratory, 1980, Argonne (unpublished), p. 45.
[13]A. E. Livingston, in Proceedings of the Workshop on Foundations of the Relativistic Theory of Atomic Structure, Argonne National Laboratory, 1980, Argonne (unpublished), p. 286.
[14]A. M. Desiderio and W. R. Johnson, Phys. Rev. A 3, 1267 (1971).
[15]J. B. Mann and W. R. Johnson, Phys. Rev. A 4, 41 (1971).
[16]K. T. Cheng and W. R. Johnson, Phys. Rev. A 14, 1943 (1976).
[17]K.-N. Huang, M. Aoyagi, M. H. Chen, B. Crasemann, and H. Mark, At. Data Nucl. Data Tables 18, 243 (1976).
[18]M. H. Chen, B. Crasemann, M. Aoyagi, K.-N. Huang, and H. Mark, At. Data Nucl. Data Tables 26, 561 (1981).
[19]S. J. Brodsky and P. J. Mohr, in *Structure and Collisions of Ions and Atoms,* edited by I. A. Sellin (Springer, Berlin, 1978), p. 3. Recent calculations of the self-energy of the $1S_{1/2}$ state have been reported by J. Sapirstein, Phys. Rev. Lett. 47, 1723 (1981), and G. Soff, P. Schlüter, B. Müller, and W. Greiner, Phys. Rev. Lett. 48, 1465 (1982).
[20]A. R. Edmonds, *Angular Momentum in Quantum Mechanics* (Princeton University, Princeton, N.J., 1960).
[21]M. E. Rose, *Relativistic Electron Theory* (Wiley, New York, 1961).
[22]These numbers have been independently calculated by W. R. Johnson, private communication, 1982.